Forecasting methods for occurrence and magnitude of proton storms with solar soft X rays

H. A. Garcia

Space Environment Center, National Oceanic and Atmospheric Administration, Boulder, Colorado, USA

Received 1 April 2003; revised 12 September 2003; accepted 29 September 2003; published 10 February 2004.

[1] Solar energetic proton (SEP) events in the vicinity of Earth have the potential of affecting the performance of civilian, military, and research satellites, including such diverse functions as communications, spacecraft operations, surveillance, navigation, and life support systems. The National Oceanic and Atmospheric Administration's (NOAA) Space Environment Center and the U. S. Air Force Weather Agency cooperate to provide advance warnings of SEP events. Their explicit duties include the need to continually upgrade and improve the accuracy, timeliness, and scope of SEP forecasts. Previous work on this topic established the empirical connection between SEPs and low-temperature X-ray flares. The main focus of the present work is to improve the quality of SEP forecasts by enhancing the size and content of the flare database used to quantify the probability model, tuning the model with imposed operational constraints, and augmenting each SEP prediction with an estimate of the magnitude of the particle event itself. *INDEX TERMS:* 7514 Solar Physics, Astrophysics, and Astronomy: Energetic particles (2114); 7519 Solar Physics, Astrophysics, and Astronomy: Flares; 7554 Solar Physics, Astrophysics, and Astronomy: X rays, gamma rays, and neutrinos; 7594 Solar Physics, Astrophysics, and Astronomy: Instruments and techniques; *KEYWORDS:* forecasting, proton events

Citation: Garcia, H. A. (2004), Forecasting methods for occurrence and magnitude of proton storms with solar soft X rays, *Space Weather*, *2*, S02002, doi:10.1029/2003SW000001.

1. Introduction

[2] Predicting the probability of solar energetic proton events (SEPs) is an essential part of space weather forecasting, considered by many users of space weather products to be of cardinal importance. The utilization of real-time GOES X-ray observations of the Sun continues to play an indispensable role in this process. Soft X rays exhibit several exploitable attributes in this regard, one being the unexpected phenomenon that anomalous low flare temperatures are empirically related to the occurrence of energetic proton enhancements in interplanetary space. This is a very implementable relationship that can be readily automated to the degree that SEP probabilities can be computed and posted without human intervention [*Garcia et al.*, 1999].

[3] One of the main attributes of the method is that it produces immediate, real-time predictions. At SEC the algorithm operates continuously, monitoring the solar X-ray output at a 1-min cadence (twenty 3-s measurements), remembering the time of flare onset, computing the temperature and emission measure from the time that flare detection is confirmed, and at the moment that the temperature and $1-8$ $\AA$ flux have peaked, computing the SEP probability and relaying this information to the Space Weather Operations Center. Thus the forecaster has this information at his disposal even before the flare has ended.

[4] The principal shortcomings of the method are the number of failed SEP forecasts that occur, either because some actually occurring SEPs are underpredicted, or because predicted SEPs do not occur or do not meet the threshold criteria. The method also suffers from the same insurmountable problem affecting all SEP forecasting schemes: very energetic particle events may reach the vicinity of Earth in a very short time period, in some exceptional cases making forecasts of SEP onset virtually irrelevant. During the reporting period of this paper, five particle events impacted the Earth in less than 40 min from flare onset. Elapsed time, reckoned from flare maximum to SEP onset, barely exceeds light time in some exceptional cases, which allows even less time for reaction. The described methodology requires that the flare maximize before the prediction algorithm may operate. Moreover, the largest, most disruptive events host the highest energy particles which are the first to arrive and are, consequently, the least amenable to advance warning. However, most extreme particle events are usually preceeded by large flares which tend to ramp up quickly, giving the alert forecaster some additional forewarning to condition his forecast as the flare continues to develop. Most SEPs follow the flare with a sufficient lag time that a forecast issued at the time of flare maximum has great relevance.

[5] The present work is dedicated in part to improving SEP forecasts by utilizing a greatly expanded database consisting of $1460 \geq$ M1 flares to modify the basic mathematical algorithm and by tuning the process with newly devised constraints, defined to optimally minimize the number of misses and false alarms. The second purpose

of this work is the heuristic investigation of other observables in the X-ray domain that pertain to the magnitude of the SEP event itself. It is found that certain properties of the flare; namely, temperature, maximum X-ray intensity, flare duration, and especially emission measure all independently correlate to varying degrees with the intensity of the proton event and when combined in a single solution, can provide a means for improving its evaluation. Finally, certain combinations of hard X-ray and soft X-ray energy fluxes provide additional signatures for predicting SEP occurrence.

[6] The paper is organized as follows: section 2 presents a brief review of the extant literature pertaining to various phenomena related to SEP occurrence, including those papers dedicated to SEP forecasting. Section 3 contains a reprise of the empirical evidence for a SEP-flare temperature association. Section 4 describes the SEP prediction algorithm based on low temperature flares, upgraded from previous results by a newly constructed database. Section 5 presents a statistical summary of results, including the efficiencies obtainable from special constraints. Section 6 outlines the search for alternative soft X-ray signatures for quantifying SEP magnitude. Section 7 reveals an entirely new predictor for SEP occurrence involving a combination of both soft and hard X-ray measurements and the final section discusses merits of heuristic investigations such as those described in this paper vis a vis the ''Big Flare Syndrome'' for forecasting solar related geoeffective events.

2. Characteristics of Solar Energetic Proton (SEP) Associated Flares and Related Phenomena

[7] Solar flares that associate with energetic particle events display a number of distinguishing features. These flares are generally characterized by smooth, long duration light curves in soft X rays (and occasionaly in hard X rays), large loop structure, and spectral hardening in hard X rays [*Garcia*, 1994a; *Kiplinger*, 1995; *Garcia and Kiplinger*, 1996]. The relationship between SEPs and long duration soft X-ray flares is one of the earliest recognized features in this regard. *Cliver et al.* [1983] also noted the paucity of an impluse in proton-associated flares. *Cliver and Cane* [1989] discriminated impulsive from gradual soft X-ray flares by their e-folding decay time. *Cane et al.* [1986] further classified energetic particle events by the parent flare: impulsive or long duration (namely,impulsive flares are short duration, electron-rich, and proton-poor, rarely produce interplanetary shocks but often associate with meter wavelength type III radio bursts, while long-duration soft X-ray flares are generally proton-rich, electron-poor, produce strong interplanetary shocks, and associate with type II and type IV radio bursts). They attributed the two classes of particle event to different flare acceleration processes. We now associate the above described properties of ''long duration'' flares to SEP-associated flares (hereinafter SEP flares).

[8] However, more than 2 decades of solar research has demonstrated that SEPs also associate with a variety of phenomena other than flares, principally coronal mass ejections (CMEs), interplanetary shocks, filament eruptions, centimetric and metric type II radio bursts, and nuclear gamma rays. *Kahler et al.* [1978] advanced the proposition that coronal mass ejections are a necessary condition for the occurrence of a prompt proton event. From that time forward the CMEs and their concomitant shocks in large proton events have gained increasing acceptance as the primary driver [*Kahler et al.*, 1984; *Cane and Stone*, 1984; *Kahler*, 1987; *Cane et al.*, 1988; *Kahler*, 1993; *Reames et al.*, 1996]. The possibility that filament eruptions may have a key role in the generation of energetic protons has also been considered, particularly in those cases where no flare or CME was observed [*Kahler et al.*, 1986; *Bai*, 1986a, 1986b]. *Akinyan et al.* [1980] and *Kahler* [1982] independently found a relationship between the duration of microwave bursts and strong SEP events.

[9] The above citations pertain primarily to scientific investigations relating various physical phenomena to the production of energetic particle events. They do not address the specific problem of predicting SEPs in the vicinity of Earth. Most papers dedicated to SEP forecasting were presented in a workshop format. *Balch* [1999] and *Kunches and Zwickl* [1999] presented at the 1997 Radiation Measurements workshop at the Johnson Space Flight Center in Houston, Texas. Earlier papers were presented at Solar Terrestrial Prediction Conferences: at Muedon, France (1984) [*Pereyaslova et al.*, 1984; *Miroshnichenko*, 1984; *Balch and Kunches*, 1986]; at Ottawa, Canada (1992), [*Shea and Smart*, 1993]; and at Hitachi, Japan (1996) [*Lin and Zheng*, 1997; *Kunches and Zwickl*, 1997].

[10] It is now commonplace to relegate flares to a less prominent role in SEP generation, subordinate to CME-driven shocks both inside the solar corona and in interplanetary space. However, as the following discussion will show, flares exhibit a high degree of empirical association with respect to both SEP incidence and magnitude. These findings suggest a significant contributory role of moderate to large flares in most occurring SEPs, although the exact nature of this role is unclear at this time.

3. The Association of SEPs to Low-Temperature Soft X-Ray Flares

[11] Specifically, the feature exploited in the present work is the tendency of SEP flares to have anomalous low temperature in soft X rays. (Methods for calculating flare temperature using full disk soft X rays are described by *Garcia* [1994b].) The primary database for this study was compiled from GOES 8 and GOES 10 X-ray observations accumulated between January 1988 and April 2002.

[12] Figure 1 shows the distribution of peak flare temperature with respect to peak logarithmic X-ray flux. (Peak temperature always precedes or is concurrent with peak flux.) This plot reveals several prominent features that characterize the temperature versus X-ray intensity relationship: On average, temperature increases monotonically with increasing X-ray intensity; SEP flares (diamonds in Figure 1) occupy a lower temperature stratum than normal flares (dots in Figure 1). The partially overlapping temperature distributions, fitted with quadratic functions,

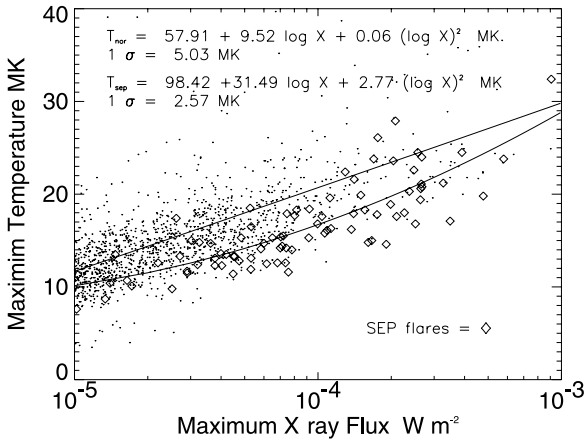

Figure 1. Flare temperature distribution with respect to X-ray flux.

appear to merge approximately at the X-ray intensities of M1 ($10^{-5}Wm^{-2}$) and X10 ($10^{-3}Wm^{-2}$) and diverge at midrange; the incidence density of normal flares thins out at higher X-ray intensities, while SEP flare densities remain nearly uniform over the full logarithmic intensity range (above M1) except for a pronounced weakening near the upper and lower limits; and the total number of normal flares exceeds the number of SEP flares by a large factor, roughly 40:1.

[13] Each temperature distribution was fitted with a quadratic polynomial for all ≥M1 flares. The normal flare temperature distribution turns out to be virtually linear as shown on the plot and as indicated by the quadratic coefficient (equation (1)); the SEP flare distribution is significantly nonlinear (equation (2)).

$$T_{nor} = 57.9 + 9.52\,log(X) + 0.06\,(log(X))^2\ MK \qquad (1)$$

$$T_{sep} = 98.4 + 31.5\,log(X) + 2.77\,(log(X))^2\ MK \qquad (2)$$

Clearly, neither of these numerical fits is valid below M1 intensities: equation (1) because the temperature curve of normal flares tends to flatten for very weak flares and does not fall much below 6 *MK* even for A class flares [see *Feldman et al.*, 1996, Figure 6], and equation (2) because SEP incidence falls sharply below M3 intensity and is virtually negligible below M1. The M2.8 ($2.8 \times 10^{-5}Wm^{-2}$) intensity level appears to be the lower X-ray boundary of high SEP incidence (see discussion in section 5).

4. Logistic Regression Probability Model

[14] The SEP occurrence probability model is statistically based, encompassing a large population of flares with widely ranging temperatures and intensities where the principal model input consists of binary responses (either a SEP was observed following a flare or none was observed). Probability, expressed as a linear combination of terms, would be inconsistent with the laws of probability. However, a statistical analysis, known as logistic regression, associates each binary outcome with a set of environmental variables and probability (0 to 1) can be expressed in the following form [*Garcia*, 1994a]:

$$P(X,T) = \frac{e^{\eta}}{(1+e^{\eta})}, \qquad (3)$$

where, in this case, the real function η (equation (4)) is a linear combination of two environmental variables: temperature T and X-ray flux X and includes a constant term, separate X and T terms, and an interaction term,

$$\eta = C_0 + C_1\,log(X) + C_2 T + C_3\,log(X) \times T. \qquad (4)$$

T is an intermediary parameter related to the observed T_o, X and the probability, P, [*Garcia et al.*, 1999]

$$T = T_o + 4P(3 + log(X)). \qquad (5)$$

[15] The coupled equations are solved iteratively to arrive at a unique value of P. The result may be used either to solve numerically for the probability of a single observed [X, T_o] vector or to construct a family of curves representing probability contours of all ranges of $X \geq$ M1 and T_o. In the latter case the plot provides a convenient means for manually interpolating probabilities.

[16] Newly derived coefficients of the environmental terms obtained from the expanded database are shown in Figure 2 where probability contours are superimposed

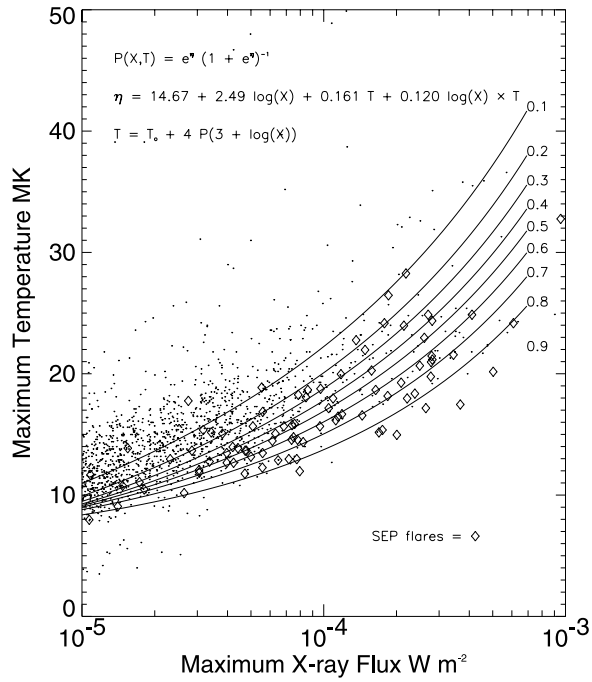

Figure 2. Low flare temperature probability model and probability contours.

on the same temperature distributions shown in Figure 1. It is seen that a small population of low-temperature, non-SEP associated flares occurred in the high-probability zone at $\leq$M3 X-ray intensities even though the great majority of low intensity flares were well below the 50% probability level. Additionally, a small number of non-SEP-associated flares in the high-probability zone are seen at higher intensities. The latter, without exception, were flares that occurred either on or beyond the solar limb or at far eastern central meridian distances.

[17] The location of the active region (beneath the flare where main X-ray emission is presumed to originate) has a profound influence on the interplanetary trajectory that energetic particles will take after they leave the vicinity of the Sun, and therefore, on the likelihood that they may be observed in the vicinity of the Earth. The central meridian distance (CMD) of the active region was included as an additional term in the original form of the environmental variable equation [*Garcia*, 1994a, equation (5)], where the term was activated for CMDs east of E40 and omitted for CMDs west of E40. However, this procedure lacked flexibility in accounting for position-dependent variability of other locations, particularly those further to the east. It was later determined that a more positive means to accommodate for location was to include it as a constraint whose quantitative effect on SEP probability may be adjusted to account for varying CMDs. These problems are discussed in section 6.

5. Summary of Results

[18] The source database is comprised of approximately 1460 $\geq$ M1 flares occurring mostly in solar cycles 21, 22, and the first half of cycle 23. During the same period 87 SEP events (defined as $\geq$10 particles cm^{-2} sr^{-1} s^{-1} for $\geq$10 MeV protons sustained for $\geq$15 min) were officially registered by Space Environment Center's Space Weather Operations.

[19] Two categories of flares were omitted from the study because their computed temperatures were of doubtful accuracy: 16 saturated flares that exceeded the dynamic range of the X-ray detectors in one or both channels and 90 flares that occurred on or beyond the solar limb. Two hundred fifty one flares of unknown location were also not included because, as noted above, the active region CMD often influences SEP observability and thus may have a negative impact on the study results and conclusions. Consequently, the basic data set included 1103 flares covering all $\leq$90° CMDs and all $\geq$M1 flares.

5.1. Special Constraints

[20] At the most basic level the success of most prediction schemes may be measured in terms of four parameters that encompass all outcome aspects of the predictive process. These parameters are organized in a 2 $\times$ 2 matrix, popularly known as a contingency table, where the elements are number of true positive predictions "hits," the number of untrue positive predictions "false alarms," the number of untrue negative predictions "misses," and the number of true negative predictions. The main objective, of course, is to maximize the number of true and minimize the number of untrue predictions. The statistical outcome of the predictive process may be influenced beforehand by the defined conditions that constitute a "positive" prediction. A too relaxed set of criteria may increase the number of hits, but it will also increase the number of false alarms. A too restrictive set will minimize the false alarms but it will increase the number of misses. A proper balance between these alternatives may be sought by introducing an objective scoring system into the process to maximize the overall forecasting efficiency.

[21] In the present case four arbitary constraints were considered: (1) Relax 'hit' criterion, P, to less than 50%, (2) Eliminate active regions (ARs) at large easterly CMD, (3) Eliminate low M class flares, and (4) Eliminate low P $\times$ Δt products (defined below). The first three constraints are natural selections based on prior experience; the fourth, P $\times$ Δt, was discovered through experimentation. *P* is the probability defined by equations (3)–(5), and Δt is the flare duration defined here as the elapsed time between onset and the time when the 0.5–4 $\AA$ flux decreases to 25% of its peak value.

[22] Two cases, i.e., two levels of the affected criterion, were considered for each constraint where the two levels of the first constraint (hit criterion) is repeated in all three contingency tables (Figure 3), beginning with the second constraint.

[23] The results are scored by subtracting misses and false alarms from hits. Misses that were incurred from previous constraint criteria must also be subtracted in reckoning each score to account for cumulative misses up to that point. Thus the merit factor, or score, has the following form: $S = h - m - f$ (all misses by default). In the final analysis the most positive (least negative) score "wins."

5.2. Contingency Tables

[24] It is seen that in all cases *S* is negative; the sum of misses and false alarms always exceeds the number of hits. The hit criterion by percent of probability is a very arbitrary measure of success since it is based on a model which is itself subject to interpretation. Thus reducing this criterion to 40% to boost the number of hits, as indicated in the contingency tables, may carry greater weight from the viewpoint of the forecaster than the detrimental effect of a greater number of incurred false alarms. Significant benefits, too, are derived from avoiding far eastern CMD flares and weak flares. Current practice recognizes the former in most cases but not the latter. As noted in section 2, the number of SEP incidence falls sharply below M2.8 but flares in this intensity range may have exceptionally low temperature and thus generate very high computed SEP probabilities in the context of the adopted logistic model. In the case of $\leq$M2.8 flares the number of generated false alarms significantly outnumbers the number of SEP flares in this intensity range; this disparity increases at an even greater rate for $\leq$M1 flares as demonstrated by previous experimentation (not described).

Contingency Tables for Active regions					
All longitudes&All classes			Longitudes W of E45		
n = 1103			n = 849 8 misses		
Hit criterion 50%			Hit criterion 50%		
S = h-m-f =-112			S = h-m-f-8 =-101		
	SEP	NoSEP		SEP	NoSEP
Pred	46	123	Pred	41	102
NoPred	35	899	NoPred	32	674
Hit criterion 40%			Hit criterion 40%		
S = h-m-f =-124			S = h-m-f-8 =-106		
	SEP	NoSEP		SEP	NoSEP
Pred	57	158	Pred	50	126
NoPred	23	865	NoPred	22	651

Contingency Tables for Weak Flares					
All flares $\geq$ M2			All flares $\geq$ M2.8		
n = 551 6 misses			n = 422 10 misses		
Hit criterion 50%			Hit criterion 50%		
S = h-m-f-8-6 =-70			S = h-m-f-8-10 =-61		
	SEP	NoSEP		SEP	NoSEP
Pred	38	66	Pred	38	55
NoPred	28	419	NoPred	26	303
Hit criterion 40%			Hit criterion 40%		
S = h-m-f-8-6 =-72			S = h-m-f-8-10 =-60		
	SEP	NoSEP		SEP	NoSEP
Pred	48	88	Pred	48	74
NoPred	18	397	NoPred	16	284

Contingency Tables for low P×Δt					
P×Δt $\geq$20			P×Δt $\geq$30		
n = 121 10 misses			n = 98 15 misses		
Hit criterion 50%			Hit criterion 50%		
S = h-m-f-8-8-10 =-45			S = h-m-f-8-8-15 =-39		
	SEP	NoSEP		SEP	NoSEP
Pred	37	39	Pred	37	33
NoPred	17	28	NoPred	12	16
Hit criterion 40%			Hit criterion 40%		
S = h-m-f-8-8-10 =-36			S = h-m-f-8-8-15 =-27		
	SEP	NoSEP		SEP	NoSEP
Pred	46	48	Pred	46	39
NoPred	8	19	NoPred	3	10

Figure 3. Contingency tables expressing the statistical outcome of constraint implementation described in text.

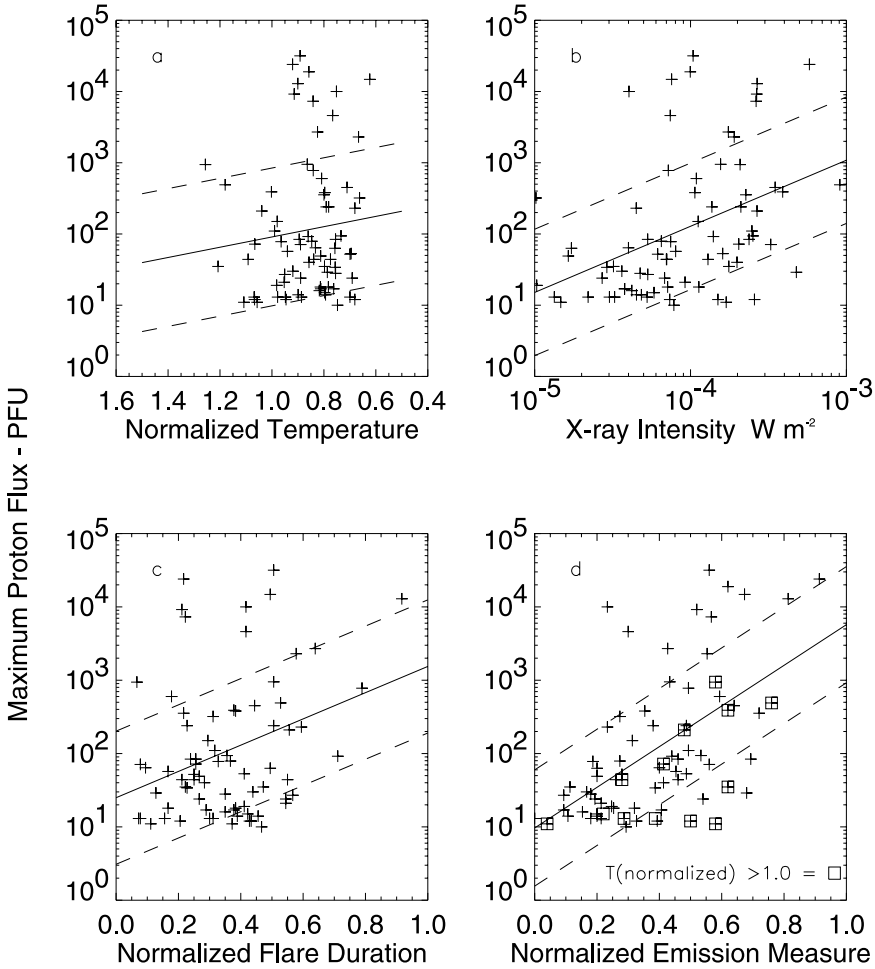

Figure 4. Scatterplots of solar energetic proton (SEP) magnitude in pfu versus temperature, X-ray intensity, flare duration, and emission measure. Squares in emission measure plot indicate higher than average temperature flares. Temperature is normalized by dividing each observed temperature by the average temperature at that X-ray intensity (equation (1)); duration is normalized by dividing Δt in hours by 3; emission measure is normalized by subtracting 49.5 from the observed logarithm and dividing by 1.5.

The contingency table for weak flares incorporates the CMD $\leq$ *E*45 criterion as do all subsequent tables.

[25] A heuristic study of various other observed, derived and combinatorial parameters in the X-ray domain found that low values of the product, probability $\times$ flare duration were correlated with false alarm flares. Approximately 25% of false alarm flares had P $\times$ Δt $\leq$ 30 whereas all hit flares were above this level. The contingency table for P $\times$ Δt incorporates the weak flare criterion for $\geq$M2.8. These cumulative findings and how they may be used to benefit the space weather forecaster are discussed further in section 10.

6. Determining SEP Magnitude

[26] Several X-ray related parameters were investigated for possible connections with SEP magnitude: namely, flare temperature, X-ray intensity, flare duration, and emission measure. (Methods for determining flare emission measure are described by *Garcia* [1994b].) Figure 4 contains scatterplots of these four parameters with respect to SEP magnitude, measured in particle flux units pfu (1 pfu = particle sec^{-1} cm^{-2} sr^{-1}). In each plot of Figure 4, the solid line depicts the fitted SEP sensitivity gradient, and dashed lines indicate the 1σ boundry. Where practical these parameters have been normalized (see Figure 4 caption) in order to make the plots mutually comparable.

[27] Despite being strongly correlated with SEP occurrence, temperature (top left of Figure 4) exhibits the weakest correlation with respect to SEP magnitude among the parameters tested. (Note that the normalized temperature is scaled inversely, i.e., high to low, analogous to its inverse relationship with respect to SEP occurrence.) On the other hand, emission measure (EM) (bottom right of Figure 4) which is not (or weakly) correlated with SEP occurrence, has the strongest SEP magnitude correlation. X-ray intensity

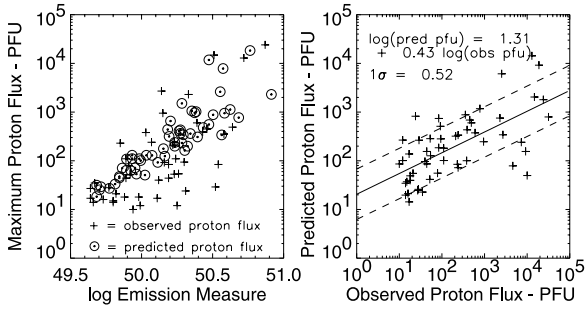

Figure 5. (left) Proton flux ensemble solution. Emission measure, X-ray intensity and flare duration are combined to obtain a single expression for SEP magnitude. Proton flux in pfu is plotted versus EM, the dominant parameter. (right) Predicted versus observed proton flux. Dashed lines delineate the one standard deviation limits of this dispersion.

(top right of Figure 4) and flare duration (bottom left of Figure 4) apparently fall between these extremes.

[28] Although the emission measure is clearly the dominant parameter respecting SEP magnitude, a small number of low magnitude SEPs occurred at midrange EM. The majority of the latter, outside and below the 1σ boundry, however, were high-temperature flares, normalized T ≥ 1.0 (designated by small squares). These higher-than-average temperature events were excluded from the following combined parameter solution (below).

[29] Combining three parameters into one solution yields a distinctly more robust association with SEP magnitude than does any one parameter by itself. (Temperature was not included owing to its relatively weak correlation.) The combined solution plot, Figure 5 (left), is cast into the horizontal frame of the dominant parameter, EM. In this frame the crosses represent observed EM, and circles represent predicted values. The final parameter formulation is expressed as a linear combination of terms where the numerical coefficients were obtained by least squares:

$$\Phi = -115.67 + 2.34EM - 1055X + 0.44\Delta t, \qquad (6)$$

where Φ is log PFU, *EM* is log emission measure, *X* is 1–8 Å X-ray flux in Wm^{-2}, and Δ*t* is flare duration in hours. (See section 5 for definition of flare duration.)

[30] Figure 5 (right) plots the predicted proton flux against the observed flux where the logarithmic dispersion deviation 1σ = 0.54 is equivalent to a factor of 3.3. Approximately 25% of the points fall outside these limits.

[31] The fact that EM = n^2V, indicative of the plasma source's mass and volume, suggests that flares may contribute to the generation of proton events by supplying a seed population of energetic particles.

7. A Composite Hard X-Ray–Soft X-Ray SEP Predictor

[32] Hard X-rays in combination with soft X rays were further investigated for a possible connection with either SEP occurrence or SEP magnitude. No significant correlation with SEP magnitude was found in this regard (except as noted below), but when the lower-energy 20–70 keV hard X-ray channels (in the thermal regime) were plotted versus the 1.5–12 keV (1–8 Å) soft X-ray passband a distinct signature for SEP occurrence was evident. The hard X-ray data for this test was obtained from the HXRS experiment [*Garcia et al.*, 1998] aboard the Department of Energy MTI satellite launched in March 2000.

[33] Figure 6 contains plots of the four lowest HXRS energy channels, 12–29, 19–29, 29–44 and 44–67 keV, versus the softest GOES X-ray band. These plots in Figure 6 demonstrate that the hard X-ray flux of the majority of SEP flares (small squares) at all soft X-ray intensities above a certain minimum, roughly ≥M3, lies below an arbitrarily diagonal boundary drawn across this parameter space. Contrarily, the hard X-ray flux of the great majority of normal (crosses in Figure 6) flares lies above this boundry. In the minority of SEP flares that lie above (and left) of the boundries, the SEP magnitudes are, without exception, ≤50 pfu, i.e., weak particle events. This empirical relationship appears not to hold in the case of higher energy, nonthermal hard X-rays; channel 44–67 keV is only marginally useful in this regard.

[34] The exact reason for this behavior is unknown at this time; however, it is known that flares that are associated with energetic ions are electron-poor [*Fletcher*, 2002]. This property, namely, the electron-poor property

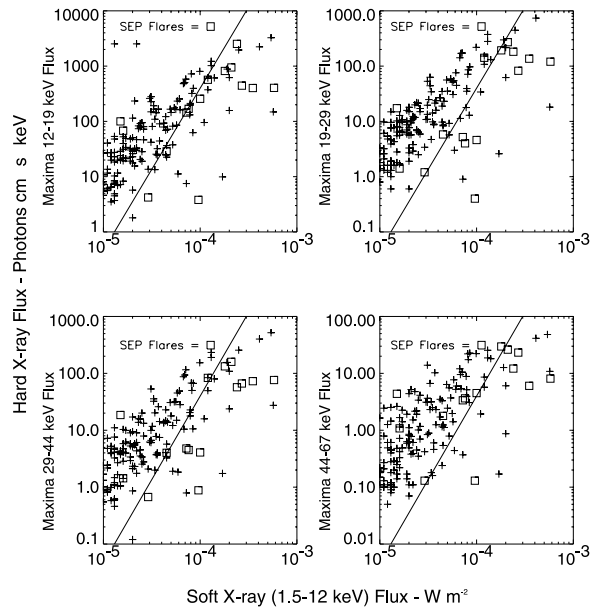

Figure 6. Concurrent hard and soft X-ray measurements in four hard X-ray passbands provide an independent signature of SEP occurrence. Diagonal lines are arbitrarily drawn separating the majority of SEP (squares) from the majority of normal (crosses) flares. Largest SEP events lie to the right and weakest SEP events to the left, providing a rough measure of SEP magnitude.

Table 1. Extreme X Ray Flares

Cycle 21						Cycle 22					
Year	Date	Time	Mag	CMD	SEP	Year	Date	Time	Mag	CMD	SEP
1978	10 Jul.	0616	X8	E58	no	1989	6 Mar.	1401	X13	E90	yes
1978	11 Jul.	1052	X20	E46	no	1989	17 Mar.	1738	X7	W57	yes
1979	18 Aug.	1413	X6	E99	yes	1989	16 Aug.	0059	X15	E84	no
1979	19 Sep.	2304	X5	E33	no	1989	29 Sep.	1125	X10	W97	yes
1980	6 Nov.	0336	X9	E74	no	1989	19 Oct.	1256	X14	E10	yes
1982	3 Jun.	1143	X8	E72	yes	1989	24 Oct.	1815	X6	W57	yes
1982	4 Jun.	1332	X6	E55	no	1990	21 May	2215	X6	W30	yes
1982	6 Jun.	1633	X10	E26	yes	1990	24 May	2048	X9	W78	yes
1982	9 Jul	0739	X10	E73	yes	1991	25 Jan.	0631	X11	E78	no
1982	12 Jul.	0947	X7	E37	no	1991	4 Mar.	1400	X7	E99	no
1982	15 Dec.	0200	X13	E24	yes	1991	7 Mar.	0749	X6	E66	no
1982	17 Dec.	1854	X10	W21	no	1991	22 Mar.	2244	X10	E28	yes
1984	25 Apr.	0001	X12	E43	yes	1991	25 Mar.	0810	X5	W08	no
1984	20 May	2234	X10	E52	no	1991	1 Jun.	1503	X16	E96	no
						1991	4 Jun.	0343	X15	E70	yes
						1991	6 Jun.	0104	X15	E44	no
						1991	9 Jun.	0139	X10	E04	no
						1991	11 Jun.	0203	X12	W17	no
						1991	15 Jun.	0815	X15	W69	yes

of SEP flares, is consistent with weak hard X-ray thermal Bremsstrahlung emission vis a vis soft X rays of this flare species as demonstrated by these results. As in the case of other heuristically founded phenomena discussed in this paper, this finding represents a new exploitable space weather tool, the present lack of a firm theoretical basis notwithstanding.

8. The Case Against Extreme X-Ray Flares and SEPs

[35] This paper has emphasized the importance of heuristic investigations in pursuit of exploitable phenomena, primarily in the X-ray domain, for the prediction of energetic particle events in the vicinity of Earth. Heretofore, predictive schemes have relied heavily on the association between SEPs and extreme X-ray flares. Table 1 lists the extreme flares (flares that saturated one or both GOES X-ray channels) occurring during solar cycles 21 and 22, clearly indicating that the very large X-ray flares that did not result in SEPs observed at Earth originated mostly from active regions at far eastern CMDs (suggesting that energetic protons were generated by these flares but missed the Earth). But a significant number of large flares that did not result in SEPs (4 out of 10) occurred at western CMDs or near Sun center, indicating that this association is far from perfect. It is true, however, that at least two of the latter (17 December 1982 and 9 June 1991) may have resulted in a particle enhancement but were not reported because a SEP was already in progress. Three far eastern CMD SEP-less flares also fell into this catagory. (NOAA does not report new SEP occurrences while a SEP is still in progress.)

[36] Furthermore, it is not clear that all of the large, far eastern SEP-less flares actually produced energetic protons. *Cliver and Cane* [1989] stated that the likelihood of a visible (meaning very intense) disk flare, "giving rise to a significant proton event was not strongly dependent on flare location. Only the M-class and C-class proton parent flares exhibited a clear preference to occur west of the solar central meridian."

[37] Some moderate-sized flares are known to have been associated with some very large SEP events. Figure 7 shows the distribution of SEP events binned according to NOAA flare class and particle event magnitude, expressed in PFUs. As expected, the population of small SEPs, PFU $\leq$100, are associated with predominately M-class flares. Between 100 and 10,000 PFUs X-class flares are the major contributors; however, at the most extreme levels the distribution appears to be almost uniform across all flare classes above M6, demonstrating that moderate-sized flares can also be potent sources of largest particle events.

[38] These facts are emphasized to demonstrate the need for alternative means, usually heuristic, for the discovery of new and independent signatures within the X-ray record and external to it that correlate with SEP occurrence and SEP magnitude. These discoveries can often lead to new insights regarding flare physics and the generation of energetic particles in particular.

9. Discussion and Conclusions

9.1. Employing Constraints

[39] Section 5 devoted to special constraints endeavored to quantify the rewards and penalties incurred by applying various criteria to the selection process. It was found that a mechanical, objective scoring system could achieve a reasonable balance between hits, misses, and false alarms, however deliberately biased toward increasing the number of hits.

[40] This is not to suggest that far eastern CMD, $\leq$M3 and $P \times \Delta t \leq 30$ flares should be totally disregarded since SEP flares sometimes do occur in these ranges.

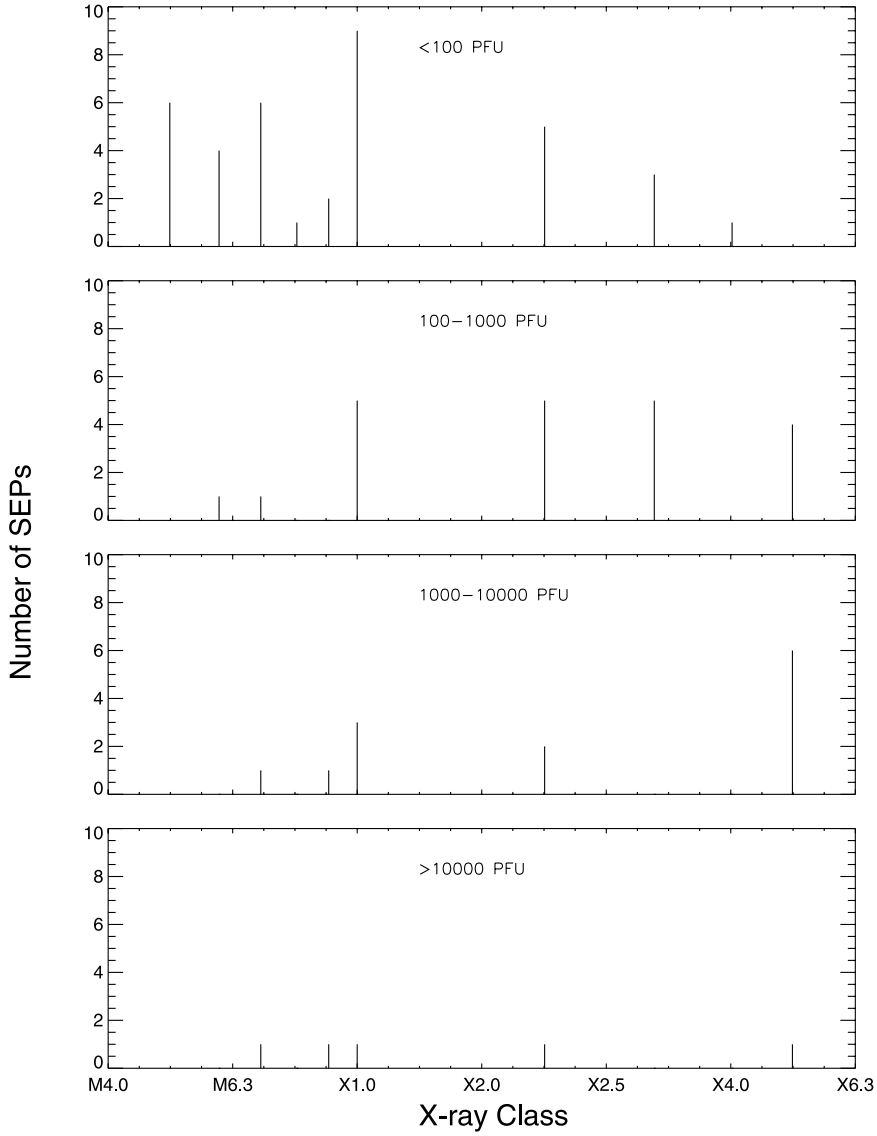

Figure 7. Histogram representation of SEP frequencies at various ascending magnitudes and binned according to flare class.

Rather, it is suggested that flares that fall into these zones are less likely to produce proton events and should be treated with considerable caution. Space weather forecasters are presented with a large number and variety of phenomena spanning the electromagnetic spectrum from decametric radio to gamma ray frequencies. Their forecasts consider all data types in assessing the imminence and magnitude of an energetic particle event. X-ray and CME observations have proven to be of particular importance in this regard. However, because of the urgency and complexity connected with the process it is helpful to provide the forecaster with a small number of partially reduced, quantitative assessments pertaining to individual pieces of this conundrum. In the present case it seems reasonable to apply a linear sliding scale to each constraint to decrement the computed probability by an amount proportional to the extent of the criterion violation,

$$\Delta P = (value - criterion) \div criterion \times P_{computed}. \quad (7)$$

A probability decrement equation must be crafted to suit each constraint, for example, if observed X-ray intensity were M1.2 and the computed probability were 55%, the probability correction would be,

$$\Delta P = (1.2 - 2.8) \div 2.8 \times 55 = -31\%. \quad (8)$$

The adjusted probability would be 24%. Similar equations may be formulated in cases where the X-ray class $\leq M2.8$, or $P \times \Delta t \leq 30$, or CMD $\geq E45^{\circ}$.

9.2. Conclusions

[41] (1) Low temperature soft X-ray flares are associated with SEP events at all X-ray intensities ≥M1; however, this empirical relationship is weak below M2.8 owing to 'false alarms' and weak above X3 owing to misses. (2) The present algorithm for forecasting SEPs from anomalous low temperature flares can be made more efficient (fewer misses and false alarms) with the application of associated constraints. (3) Rough estimates of SEP magnitudes are now possible by a procedure that incorporates emission measure, X-ray intensity and flare duration in a single formulation. (4) A combination of concurrent hard and soft X-ray flux measurements appear to provide an additional means for predicting SEP occurrence. (5) SEP signatures are found in mid-range M class flares as well as large flares which suggests that the magnitude of the flare, while important, may not be be the principal driver or best predictor of energetic protons. (6) Large to extreme X-ray flares provide no guarantee that a SEP will ensue, or that if the SEP does occur that it will be large. (7) While it may be true that fast CMEs are the principal driver of SEPs as frequently cited in the extant literature [*Kahler et al.*, 1984; *Kahler*, 1992; *Cliver and Cane*, 1989], the statisical evidence provided in the present work (and previous studies on the subject, see citations) also indicates that flares, displaying certain characteristics (described herein), have a roughly commensurate high SEP association, suggesting that the flare plays a definite but as yet unspecified supporting role very early in the SEP development.

References

Akinyan, S. T., I. M. Chertok, and V. V. Fomichev (1980), Quantitative Forecasts of solar protons based on solar flare radia data, in *Solar Terrestrial Predictions Proceedings*, vol. 3, edited by R. F. Donnelly, p. D-14, U. S. Dept. of Commer., Washington, D. C.

Bai, T. (1986a), Relationship between the first and second phases of solar flares, *Adv. Space Res.*, *6*, 203.

Bai, T. (1986b), Two classes of gamma-ray proton flares: Impulsive and gradual, *Astrophys. J.*, *308*, 912.

Balch, C. (1999), SEC proton prediction model: Verification and analysis, *Radiat. Meas.*, *30*(3), 231.

Balch, C., and J. Kunches (1986), SESC methods for proton event forecasts, in *Short Term Solar Forecasting, Sol. Terr. Pred. Proc.*, edited by P. A. Simon, G. Heckman, and M. A. Shea, p. 353, Natl. Ocean. and Atmos. Admin., Boulder, Colo.

Cane, H. V., and R. G. Stone (1984), Type II solar radio bursts, interplanetary shocks and energetic particle events, *Astrophys. J.*, *282*, 339.

Cane, H. V., R. E. McGuire, and T. T. von Rosenvinge (1986), Two classes of solar energetic particle events associated with impulsive and long-duration soft X-ray flares, *Astrophys. J.*, *301*, 448.

Cane, H. V., D. V. Reames, and T. T. von Rosenvinge (1988), The role of interplanetary shocks in the longitude distribution of solar energetic particles, *J. Geophys. Res.*, *93*(A9), 9555.

Cliver, E., and H. V. Cane (1989), X-class soft X-ray bursts and major proton events during solar cycle 21, in *Solar Terrestrial Predictions Proceedings*, edited by R. J. Thompson et al., Leura, Australia.

Cliver, E., S. W. Kahler, and P. S. McIntosh (1983), Solar proton flares with weak impulsive phases, *Astrophys. J.*, *264*, 699.

Feldman, U., G. Doschek, W. Behring, and K. Phillips (1996), Electron temperature, emission measure and X-ray flux in A2 to X2 X-ray class solar flares, *Astrophys. J.*, *460*, 1034.

Fletcher, L. (2002), Energetic particles in the solar atmosphere, in *10th European Solar Physics Meeting Proceeding*, Eur. Space Agency, Paris, France, 9–14 September .

Garcia, H. A. (1994a), Temperature and hard X-ray signatures for energetic proton events, *Astrophys. J.*, *420*, 422.

Garcia, H. A. (1994b), Temperature and emission measure from GOES soft X-ray measurements, *Solar Phys.*, *154*, 275.

Garcia, H. A., and A. L. Kiplinger (1996), Low temperature soft X-ray flares, spectrally hardening hard X-ray flares and energetic interplanetary protons, in *Solar Drivers of Interplanetary and Terrestrial Disturbances*, *ASP Conf. Ser.*, vol. 95, edited by K. Balasubramaniam, S. Keil, and R. Smartt, Astron. Soc. of the Pac., San Fransisco, Calif.

Garcia, H. A., F. Farnik, and A. L. Kiplinger (1998), Hard X-ray spectroscopy for proton flare prediction, in *Missions to the Sun II*, *SPIE Conf.*, vol. 3442, Int. Soc. for Opt. Eng., Bellingham, Wash.

Garcia, H. A., S. Greer, and R. Viereck (1999), Prediction solar energetic particle events from flare temperatures, in *Eur. Space Agency Spec. Publ.*, *448*, 983.

Kahler, S. W. (1982), Radio burst characterisics of solar proton flares, *Astrophys. J.*, *261*, 710.

Kahler, S. W. (1987), Coronal mass ejections, *Rev. Geophys.*, *25*, 663.

Kahler, S. W. (1992), Solar flares and coronal mass ejections, *Annu. Rev. Astron. Astrophys.*, *30*, 113.

Kahler, S. W. (1993), Coronal mass ejections and long risetimes of solar energetic particle events, *J. Geophys. Res.*, *98*(A4), 5607.

Kahler, S. W., E. Hildner, and M. A. Hollebeke (1978), Prompt Solar proton events and coronal mass ejections, *Solar Phys.*, *57*, 429.

Kahler, S. W., N. R. Sheeley, R. A. Howard, M. J. Koomen, D. J. Michels, R. E. McGuire, T. T. von Rosenvinge, and D. V. Reames (1984), Associations between coronal mass ejections and solar energetic proton events, *J. Geophys. Res.*, *89*(A11), 9683.

Kahler, S. W., E. W. Cliver, H. V. Cane, R. E. McGuire, R. G. Stone, and N. R. Sheeley (1986), Solar filament eruptions and energetic particle events, *Astrophys. J.*, *302*, 504.

Kiplinger, A. (1995), Comparative studies of hard X-ray spectral evolution in solar flares with high energy proton events observed at earth, *Astrophys. J.*, *453*, 973.

Kunches, J. M., and R. D. Zwickl (1997), Delayed onset solar energetic particle events, in *Solar Terrestrial Predictions: V*, p. 453, Natl. Ocean. and Atmos. Admin., Boulder, Colo.

Kunches, J. M., and R. D. Zwickl (1999), The effects of coronal holes on the propagation of solar energetic protons, in *Radiation Measurements 30*, Elsevier Sci., New York.

Lin, Y., and L. Zheng (1997), Solar microwave radiation flux and the short term prediction of proton events, in *Solar Terrestrial Predictions V*, p. 196, Hiraiso Sol. Terr. Res. Cent., Hitachinaka, Japan.

Miroshnichenko, L. (1984), The development of diagnostics and prediction methods of solar proton events, in *Short Term Solar Forecasting, Sol. Terr. Pred. Proc.*, edited by P. A. Simon, G. Heckman, and M. A. Shea, p. 244, Natl. Ocean. and Atmos. Admin., Boulder, Colo.

Pereyaslova, N. Mikirova, and M. Nazarova (1984), A method of forecasting solar cosmic ray events, in *Short Term Solar Forecasting, Sol. Terr. Pred. Proc.*, edited P. A. Simon, G. Heckman, and M. A. Shea, p. 220, Natl. Ocean. and Atmos. Admin., Boulder, Colo.

Reames, D. V., L. M. Barbier, and C. K. Ng (1996), The spatial distribution of particles accelerated by coronal mass ejection-driven shocks, *Astrophys. J.*, *466*, 473.

Shea, M. A., and D. F. Smart (1993), History, statistics and predictions of solar proton events, in *Solar Terrestrial Predictions Proceedings IV*, Natl. Ocean. and Atmos. Admin., Boulder, Colo.

H. A. Garcia, Space Environment Center, National Oceanic and Atmospheric Administration, 325 Broadway, Boulder, CO 80305, USA. (howard.a.garcia@noaa.gov)